Statistical properties of hollow atoms

Nathalie Vaeck[1] and Niels J. Kylstra[2]
[1]*Laboratoire de Chimie Physique Moléculaire, Université Libre de Bruxelles, 50 Avenue F. Roosevelt, B-1050 Bruxelles, Belgium*
[2]*Department of Physics, University of Durham, South Road, Durham DH1 3LE, United Kingdom*
(Received 7 November 2001; published 4 June 2002)

We investigate the statistical properties of a prototype of a ''hollow atom,'' i.e., an atom having a large number of empty inner shells. In particular, we have carried out *ab initio* calculations of the positions and widths of the $1s^2 4\ell^5$ states of nitrogen. These states give rise to a dense spectrum of strongly overlapping resonances. Due to the large number of open channels, the statistical description of the system simplifies considerably. We find that the distribution of the nearest-neighbor energy-level spacings follows a Wigner distribution, while the widths of the states are narrowly distributed about the average perturbative width.

DOI: 10.1103/PhysRevA.65.062502 PACS number(s): 31.15.Bs, 31.10.+z, 34.70.+e, 32.10.−f

I. INTRODUCTION

''Hollow atoms'' have all or nearly all electrons in excited shells. Such atomic states can be created by electron transfer in a variety of collision processes involving highly charged ions. For example, when highly charged ions collide with a metallic surface, hollow atoms are formed in front of and below the surface by resonant electron transfer [1–3]. Closely related experiments have been carried out using a thin metal foil target with straight microcapillaries [4]. Highly charged ions passing through the capillary are neutralized by electrons captured in highly excited shells. The atoms, which are expected to have preserved at least partially their hollow charge distribution as they exit the capillary, are extracted in vacuum and x-ray emission is observed. Multielectron capture can also occur during collisions involving highly charged ions and neutral atoms or molecules, resulting in the formation of hollow atoms [5,6]. For example, in collisions between Xe^{27+} and neutral Xe, up to 15 electrons are captured from the target in excited states of the projectile [7]. More recently, collisions between highly charged ions and cluster targets, in particular, fullerenes, have been the subject of experimental and theoretical investigations [8,9]. When Xe^{25+} ions interact with C_{60}, as many as 60 electrons can be involved in the charge-transfer mechanism [10].

Hollow atoms decay principally by Auger emission, and theoretical calculations of the positions and lifetimes of multiply excited states often constitute the only information available for assistance in interpreting the complex spectra that are measured. With the exception of investigations of triply excited states of lithium, the number of theoretical studies of multiply excited states is limited: calculations are difficult and time consuming since the number of states increases dramatically with the number of excited electrons and the principal quantum number of the occupied orbitals [11]. In addition, the density of states becomes very large and is characterized by irregular spectra of strongly interacting resonances. This makes such spectra amenable to a statistical description based on the random matrix theory (RMT) [12–14]. Originally developed to describe complex nuclear spectra [12,15,16], RMT has been applied to analyze a wide range of quantum systems, including atoms [17,18] and polyatomic molecules [19–21]. All have been shown to exhibit the same universal spectral fluctuations. It has also been realized that RMT provides a general framework for studying quantum manifestations of chaotic dynamics in simple systems having few degrees of freedom [14,22–24]. In particular, Rydberg states of atomic hydrogen in microwave, electric, and magnetic fields have been studied in detail [25–28].

These developments have led to a renewed interest in excited multielectron atomic systems. The Coulomb repulsion between electrons in such systems gives rise to complex spectra of strongly interacting states [17,18]. For example, doubly excited states of helium up to the $N=9$ ionization threshold have been investigated experimentally and theoretically [29–31]. As the double-ionization threshold is approached, the density of doubly excited Rydberg states as well as the interaction between the resonances increases significantly. For the Rydberg states converging to the $N=9$ threshold, an RMT analysis of the nearest-neighbor level spacing distribution displays a transition to a Wigner distribution [32]. Flambaum and co-workers [33–37] have presented detailed theoretical studies of the excited states of the Ce atom, Connerade *et al.* [38] have performed a multiconfiguration Dirac-Fock study of Sr I states arising from the excitation of the $4p$ core shell and O'Sullivan *et al.* [39] have investigated the lowest $4f \rightarrow 5d$ and $5p \rightarrow 5d$ transitions for Sm IX. In these works, a configuration-interaction (CI) approach was used, and the statistical properties of the system investigated, in particular, the nearest-neighbor energy-level spacing.

In this paper, we analyze a prototype of a highly excited system having a dense spectrum of autoionizing states. Specifically, we consider the quintuply excited $1s^2 4\ell^5\, ^2P^o$ states in neutral nitrogen and determine the distribution of the position and widths of the resonant states. The paper is organized as follows. In the following section we describe the theoretical methods used to calculate the properties of hollow nitrogen. A summary of the Feshbach projection operator formalism is given first. We then describe the Hartree-Fock-CI approach used to calculate the positions and the widths of the states. The high energy-level density and large autoionization widths give rise to overlapping resonances [40], so that a simple perturbative description of the decay process is not *a priori* valid. The calculated positions and

 ©2002 The American Physical Society

widths are then used to construct an effective non-Hermitian Hamiltonian matrix, which is diagonalized, thereby yielding the complex energies characterizing the resonant states. Our results are then discussed and compared to predictions of RMT.

II. OVERLAPPING RESONANCES

Our starting point is the nonrelativistic Hamiltonian of the atomic system, which we write as

$$H = H_0 + V, \tag{2.1}$$

with H_0 and V being the one- and two-body terms, respectively. Calculating properties of the resonant states by directly solving the time-independent Schrödinger equation is not practical, and we, therefore, proceed as follows. The $1s^2 4\ell^5\, {}^2P^o$ states are resonant or quasistationary states, so first we obtain an effective Hamiltonian for the system employing the Feshbach operator formalism. The operators P and $Q=1-P$ are introduced, which satisfy the usual projection operator relations, with the requirement that the action of P on a channel state does not change this state. In other words, the operator P projects onto the continuum states of the system while the complementary operator Q projects onto the discrete states. These operators can now be used to partition the Hamiltonian (2.1) into two effective energy-dependent Hamiltonians. In the discrete space, the required effective Hamiltonian is

$$\mathcal{H}_Q(E) = QHQ + QVPG_P^{(+)}(E)PVQ, \tag{2.2}$$

with the Green's operator defined by

$$G_P^{(+)}(E) = \frac{1}{P(E-H+i\epsilon)P}. \tag{2.3}$$

In our case, the Q subspace and P subspace are coupled by the two-body operator V and, therefore, $QHP=QVP$ and $PHQ=PVQ$. The first term of the effective Hamiltonian is simply the Hamiltonian acting in the discrete subspace. The second term represents the coupling of the discrete states to the open channels, the diagonal elements of which are the induced shifts and widths in the absence of the remaining discrete states, while the off-diagonal elements give the coupling of the discrete levels through the continuum. Since boundary conditions have been imposed on Green's operator, which correspond to outgoing waves, the second term in the Hamiltonian of Eq. (2.2) is non-Hermitian. The eigenvalue problem to be solved in the discrete subspace can then be expressed as

$$[h(E_i) - iw(E_i)]|Q\Psi_i\rangle = \mathcal{E}_i|Q\Psi_i\rangle, \tag{2.4}$$

with

$$h(E) = QHQ + QVP\left[\mathrm{P}\frac{1}{P(E-H)P}\right]PVQ,$$

$$w(E) = \pi QVP\,\delta[P(E-H)P]PVQ. \tag{2.5}$$

Here P refers to the ''principal value distribution.'' The spectrum of $\mathcal{H}_Q$ is purely discrete with the eigenstates having complex eigenvalues $\mathcal{E}_i$. In atomic units (a.u.), these eigenvalues are written as

$$\mathcal{E}_i = E_i - i\frac{\Gamma_i}{2}, \tag{2.6}$$

with the imaginary part being equal to the negative of one-half of the rate that characterizes the exponential decay of the states.

In order to obtain a solution of Eq. (2.4), the following approximations are made. First, the second term in the expression for $h(E)$ above is neglected. This amounts to assuming that the shifts induced by the coupling of the discrete states to the open channels are small compared to the typical energy spacings of the eigenstates of QHQ. This has the consequence that $h(E)$ is no longer energy dependent. Next, the energy dependence of $w(E)$ is removed by fixing the energies of the channel states in the narrow energy region of interest. How these energies are chosen is discussed below. Now, assuming that the channel states $|k,E\rangle$ satisfy $P(H-E)P|k,E\rangle=0$, we can write

$$w(E) = \pi\sum_{k=1}^{K} QV|k,E\rangle\langle k,E|VQ$$

$$\simeq \pi\sum_{k=1}^{K} QV|k,E_k\rangle\langle k,E_k|VQ, \tag{2.7}$$

with $k=1,\ldots,K$ labeling the decay channels. The problem of determining the positions and widths of the resonant states has now been reduced to an eigenvalue problem. In the following section, we discuss the model space used in our calculations.

III. CALCULATION OF DISCRETE AND CHANNEL WAVE FUNCTIONS

We follow the procedure of Vaeck and Hansen [11], who have studied the autoionization of multiply excited states in nitrogen ions using the suite of programs written by Cowan [41]. First a basis set of Hartree-Fock states for the discrete states are calculated. For the quintuply excited $1s^2 4\ell^5\, {}^2P^o$ states considered in Ref. [11], only a restricted number of configurations were retained. We have extended this calculation to the 24 configurations of the Layzer complex, which are the main interacting configurations. This results in $N=237\ {}^2P^o$ states in the $1s^2 4\ell^5$ manifold. Our basis states in the Q subspace are then expressed as a superposition of the (orthogonalized) Hartree-Fock states, $|\phi(\gamma_i LS)\rangle$,

$$|\psi_i(LS)\rangle = \sum_{j=1}^{N} c_{i,j}|\phi(\gamma_j LS)\rangle, \tag{3.1}$$

where γ_i denotes the coupling scheme and any other quantum numbers necessary to define the state. The expansion coefficients $c_{i,j}$ are obtained by solving the eigensystem

$$\mathbf{hc}_i = \epsilon_i \mathbf{c}_i \,. \tag{3.2}$$

The matrix elements of **h** are $h_{i,j} = \langle \phi(\gamma_i LS)|H|\phi(\gamma_j LS)\rangle$, with the diagonal elements being the Hartree-Fock energies, $h_{i,i} = \epsilon_i^{(0)}$. The ϵ_i are the eigenenergies of the basis states in the Q subspace. The projection operator in the discrete subspace can then be expressed as

$$Q = \sum_{i=1}^{N} |\psi_i(LS)\rangle\langle\psi_i(LS)|. \tag{3.3}$$

Due to the strong mixing, it is not possible to label the eigenvectors of the system by a set of quantum numbers corresponding to a dominant Hartree-Fock state. We note that the average energy of each of the $1s^2 3\ell 4\ell^3$ configurations lies below the $1s^2 4\ell^5$ manifold. This has the consequence that the configuration-averaged energy of every member of the Rydberg series $1s^2 3\ell 4\ell^3 n\ell$ is located below the $1s^2 4\ell^5$ configurations used here. Therefore, mixing between the Rydberg series and the $1s^2 4\ell^5$ states, encountered in other systems [42,43], does not significantly influence the system considered here.

The $1s^2 4\ell^5\, {}^2P^o$ states autoionize to 4980 possible $1s^2 3\ell 4\ell^3 \varepsilon\ell\, {}^2P^o$ channels via Coster-Kronig transitions. These transitions are by far the dominant decay channels. For the channel states, we again calculate a basis of Hartree-Fock states, $|\chi_k(\gamma_c[L_c S_c]\varepsilon_k \ell LS)\rangle$, with $k = 1, \ldots, K = 4980$ and $\gamma_c[L_c S_c]$ denoting the coupling scheme and the total symmetry of the target core. We next assume that the Hartree-Fock channel states approximately diagonalize *PHP*, i.e.,

$$\langle \chi_k|H|\chi_{k'}\rangle \simeq \delta_{k,k'} E_k \,. \tag{3.4}$$

While the interaction between some of the configurations of the channel states is sufficiently large to call into question this approximation, it greatly simplifies the calculations. The energy of the ejected electron ε_k has been chosen so that E_k corresponds to the average of the energy differences between each of the $1s^2 4\ell^5$ configurations and the corresponding target configuration. The energy of the ejected electron is determined principally by the angular momentum of the 3ℓ electron. Depending on the configuration, the energy is ≈ 0.47 a.u. for a $3s$ electron, 0.36 a.u. for a $3p$ electron, and 0.32 a.u. for a $3d$ electron.

In this Hartree-Fock approximation, the operator w now takes the form

$$w = \pi \sum_{k=1}^{K} QV|\chi_k(\gamma_c[L_c S_c]\varepsilon\ell LS)\rangle \times \langle \chi_k(\gamma_c[L_c S_c]\varepsilon\ell LS)|VQ. \tag{3.5}$$

Using the truncated expansions for the discrete and channel state spaces, the eigenvalues of Eq. (2.4) are determined by solving

$$\det(\boldsymbol{\mathcal{H}} - \mathcal{E}_i) = \det(\boldsymbol{\epsilon} - i\mathbf{w} - \mathcal{E}_i) = 0, \tag{3.6}$$

with

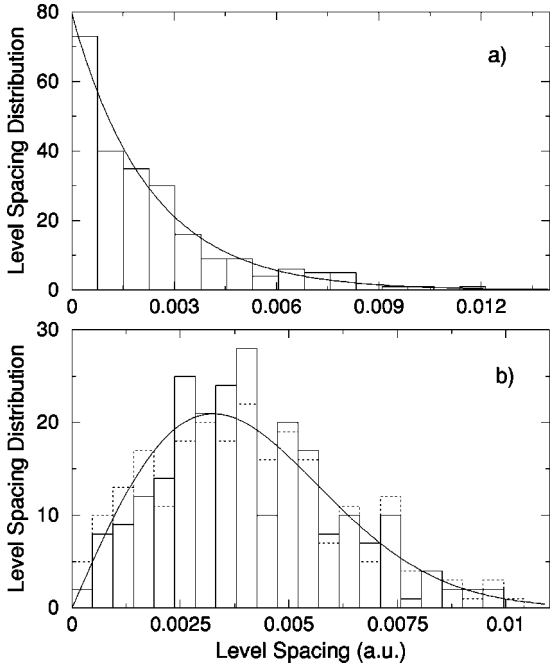

FIG. 1. Level spacing distributions. In the upper figure, a histogram of the Hartree-Fock level spacings, i.e., the spacing of the diagonal matrix elements of the Hamiltonian matrix **h** is shown. The solid curve is a Poisson distribution, with mean spacing $D = 0.002\,27$ a.u. The lower figure shows histograms of the spacing distribution of the eigenvalues of **h** (solid lines) and the real part of the eigenvalues of $\boldsymbol{\mathcal{H}}$ (broken lines). The mean spacing is the same for both distributions. A Wigner distribution (solid curve) with $D = 0.004\,08$ a.u. is also plotted.

$$(\mathbf{w})_{i,j} = \pi(\mathbf{V}^\dagger \mathbf{V})_{i,j} = \pi \sum_{k=1}^{K} (V_i^k)^\dagger V_j^k \,, \tag{3.7}$$

where

$$V_i^k = \langle \chi_k|V|\psi_i\rangle = \sum_{j=1}^{N} c_{i,j}\langle \chi_k|V|\phi_j\rangle = \sum_{j=1}^{N} c_{i,j} V_j^{(0)k} \,. \tag{3.8}$$

In the following section we investigate some of the statistical properties of the system. We begin by determining the nearest-neighbor level spacing distributions of the diagonal elements and eigenvalues of **h**.

IV. RESULTS

A. Eigenvalues in the discrete subspace

In Fig. 1 histograms of the level spacing distribution of the Hartree-Fock energies $\epsilon_i^{(0)}$ and the eigenvalues ϵ_i of the matrix **h** are shown. The distributions have been obtained by following the usual ''unfolding'' procedure (see, e.g., Ref. [23]), whereby energy spacings are determined from fluctuations about a mean cumulative energy distribution. If the energy levels of a system are not correlated, the level spacings follow a Poisson distribution

$$P(S)=D^{-1}\exp(-S/D). \tag{4.1}$$

In Fig. 1(a), a histogram of the Hartree-Fock spacing and a Poisson distribution (solid curve) with a mean spacing $D=2.3\times10^{-3}$ a.u. are shown. Good agreement between the two distributions is observed. Figure 1(b) shows a histogram of the level spacing distribution of the eigenvalues ϵ_i (solid lines) and the real part of the eigenvalues $\mathcal{E}_i$ (broken lines). We discuss the latter results in greater detail below; however, for now we note only that the mean level spacing $D=4.1\times10^{-3}$ a.u. is the same for both distributions.

The level spacing distribution for a strongly interacting, or highly correlated, system can be derived by considering a Gaussian orthogonal ensemble (GOE) of matrices. For a two-state system, one obtains the Wigner distribution

$$P(S)=\frac{\pi}{2D^2}S\exp\left(-\frac{\pi}{4}\frac{\epsilon^2}{D^2}\right). \tag{4.2}$$

This result also holds to a good approximation for systems having more than two states. Good agreement is observed between the calculated level spacing distribution and the Wigner distribution (solid curve). The distributions in Figs. 1(a) and 1(b) correspond to limiting cases of, respectively, level clustering and level repulsion. In particular, the introduction of electron-electron correlation leads a significant overall spreading of the eigenvalue distribution.

B. Matrix elements and eigenvectors

We have seen that the nearest-neighbor level spacing distribution of the $1s^2 4\ell^5$ states of nitrogen is in agreement with the spectrum expected from a GOE, in which the matrix elements are normally and independently distributed. However, in practice the distribution of matrix elements will depend on the basis used. The two-body nature of the electron-electron interaction leads to a relatively sparse Hamiltonian matrix when a basis of Hartree-Fock states is used; all the off-diagonal elements involving states differing by two or more electrons or by their grand parent coupling term are zero. For the system considered here, 44% of the matrix elements of **h** are nonzero. The structure of this matrix is shown in Fig. 2, with each point on the graph representing the location of a nonzero element. The Hartree-Fock states have been ordered by the average energy of the configurations. Figure 2 clearly demonstrates the lack of interactions between distant configurations. However, due to the large spread in the energy of the states originating from the same configuration, this structure nearly disappears when the Hartree-Fock states are ordered by their energy $\epsilon_i^{(0)}$, as is illustrated in Fig. 3.

When the zero matrix elements are discarded, the distribution of the nondiagonal Hamiltonian matrix elements is well represented by a Poisson distribution. A similar exponential decrease in the matrix element distribution was found by Flambaum *et al.* [33] for the case of the excited states of Ce. However, if we consider the matrix elements between states arising from the same configuration, the situation is different: the distribution of these 2386 matrix elements is to

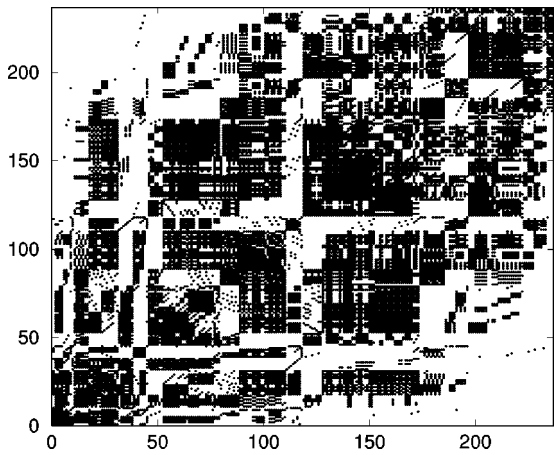

FIG. 2. The nonzero matrix elements of **h**. The matrix elements are grouped by configuration and arranged according to the average Hartree-Fock energy of the configuration. Note that 44% of the matrix elements are nonzero.

a good approximation Gaussian. We note that separating the nondiagonal matrix elements of the Hamiltonian into two sets has been proposed by Wilson *et al.* [44] in their theoretical study of the $3p^5 3d^4 \rightarrow 3p^5 3d^3 4f$ transitions in Fe VI. They showed that the distribution of the nondiagonal matrix elements between states arising from a single configuration followed a bi-Gaussian distribution, with the larger matrix elements involving basis states where the parent shell is of a common term. The system considered here has nearly no core structure, and hence the coupling scheme of the $4\ell^5$ electrons is rather arbitrary as is the choice of the parent term. For these reasons, the partition proposed in Ref. [44] does not apply.

Investigations of the distribution of the eigenvector coefficients have demonstrated ''localization,'' whereby basis states having energies $\epsilon_j^{(0)}$ within an interval $\Gamma_{\rm loc}$ centered about the eigenstate energy ϵ_i have coefficients that contribute most significantly to the eigenvector expansion. This has been discussed in, for example, Ref. [33]. In particular, for a GOE, the distribution should be Lorentzian. For banded ma-

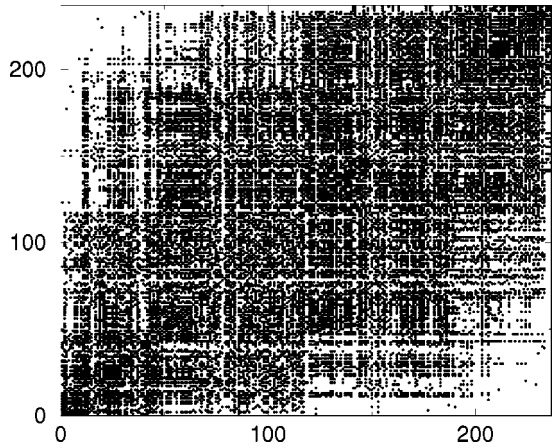

FIG. 3. The nonzero matrix elements of **h**. The matrix elements have been sorted by increasing value of their Hartree-Fock energy.

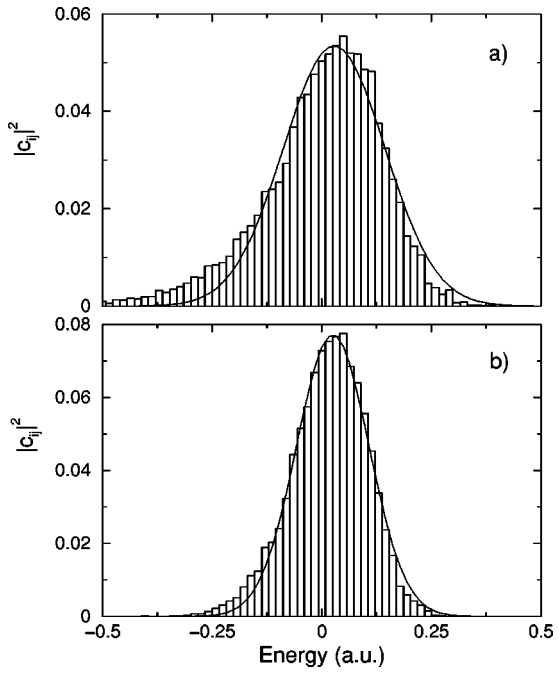

FIG. 4. Distribution of the magnitude squared of the eigenvector coefficients as a function of the energy difference between the jth Hartree-Fock basis state and the ith eigenstate of **h**. In (a) the distribution contains all of the coefficients, while in (b) only the coefficients corresponding to the 137 central eigenstates are shown. The solid curves are unnormalized Gaussian distributions with standard deviations $\sigma=0.083$ a.u. and $\sigma=0.116$ a.u., respectively. Note that the mean positions of the distributions are displaced slightly to the right of the origin.

trices, this result still holds when $|\epsilon_j^{(0)}-\epsilon_i|\lesssim\Gamma_{\rm loc}$, while a modified exponential decay for large energy separations can be expected. However, the distribution of the eigenvector coefficients, just as the distribution of the matrix elements of **h**, is basis dependent. In Fig. 4, the distribution of the magnitude squared of the eigenvector coefficients as a function of the energy difference between the jth Hartree-Fock basis state and the ith eigenstate of **h** is shown. In Fig. 4(a), the distribution of all of the coefficients is given, while in Fig. 4(b) only the coefficients corresponding to the 137 central eigenstates are shown. We find that the latter distribution is well approximated by a Gaussian distribution (solid curve), which is consistent with a Lorentzian distribution for small energy differences. The form of the wings of the distribution will depend on the ''bandlike'' structure of the Hamiltonian matrix (see Fig. 2) [33]. Note the negative skew of the distributions, which is possibly related to edge effects arising from the truncated basis. (The ''unfolded'' energy differences were not used to obtain the distribution.)

Finally, it is worth mentioning that if it is assumed that the eigenvectors are uniformly distributed on a N-dimensional sphere, the eigenvector coefficients are expected to be Gaussian distributed with standard deviation $\sqrt{N}$ [23]. For the system considered here, the coefficients $c_{i,j}$ corresponding to the central eigenstates, i.e., $i\simeq N/2$, are in fact distributed in this way.

C. Resonance widths

In the perturbative regime, the mean energy-level spacing is assumed large compared to the diagonal elements of the matrix **w**, i.e., $|\epsilon_i-\epsilon_{i\pm1}|\gg w_{i,i},w_{i\pm1,i\pm1}$. (Recall that $w_{i,i}w_{i+1,i+1}\geqslant|w_{i,i+1}|^2$.) Under these conditions

$$\mathcal{E}_i\simeq\epsilon_i-\frac{\rm i}{2}\gamma_i, \tag{4.3}$$

where $\gamma_i=2w_{i,i}$ are the perturbative widths of the discrete states. For the system considered here, the ratio between the mean width $\overline{\gamma}$ and the mean level spacing is $\overline{\gamma}/D\sim10$. This would, in general, indicate a strong coupling between the resonant states, thereby invalidating the approximation (4.3). However, the 237 $1s^24\ell^{5\,2}P^o$ autoionizing states can decay to 4980 continua. Therefore, we are in a situation where $K\gg N$, and the statistical description of the system simplifies considerably.

For a particular system the matrix element $V_i^{(0)k}$ can be positive or negative with equal probability. Hence, for K large,

$$\sum_{k=1}^{K}V_i^{(0)k}\simeq0, \tag{4.4}$$

with the variance of the distribution of the mean decreasing as $K^{-1/2}$. Let us next assume that the transition amplitudes associated with two different Hartree-Fock states are not correlated. While we know of no general physical argument to support this assumption, we point out that in our case the $K\times N$ matrix $\mathbf{V}^{(0)}$ is very sparse: each Hartree-Fock state is coupled, on average, to $\overline{K}=731$ channels (with a standard deviation of 344). This is due to the fact that V is a two-body operator, so that the only nonzero transition matrix elements are those involving Hartree-Fock discrete and channel states having the same $(4\ell)^3$ coupling scheme. It then follows that, for K large,

$$\sum_{k=1}^{K}V_i^{(0)k}V_j^{(0)k}\simeq0\quad\text{for}\quad i\neq j. \tag{4.5}$$

With this approximation

$$(\mathbf{w})_{i,j}^{(0)}=\pi\sum_{k=1}^{K}V_i^{(0)k}V_j^{(0)k}\simeq\frac{1}{2}\gamma_i^{(0)}\delta_{i,j}, \tag{4.6}$$

where the $\gamma_i^{(0)}$ are the Hartree-Fock rates. From this result and Eq. (3.7) we then obtain

$$(\mathbf{w})_{i,j}\simeq\pi\sum_{k=1}^{K}|V_i^k|^2\delta_{i,j}=\frac{1}{2}\gamma_i\delta_{i,j}. \tag{4.7}$$

Finally, Eq. (4.7) implies that the complex eigenvalues of $\mathcal{H}$ are simply

$$\mathcal{E}_i=E_i-i\frac{\Gamma_i}{2}\simeq\epsilon_i-i\frac{\gamma_i}{2}, \tag{4.8}$$

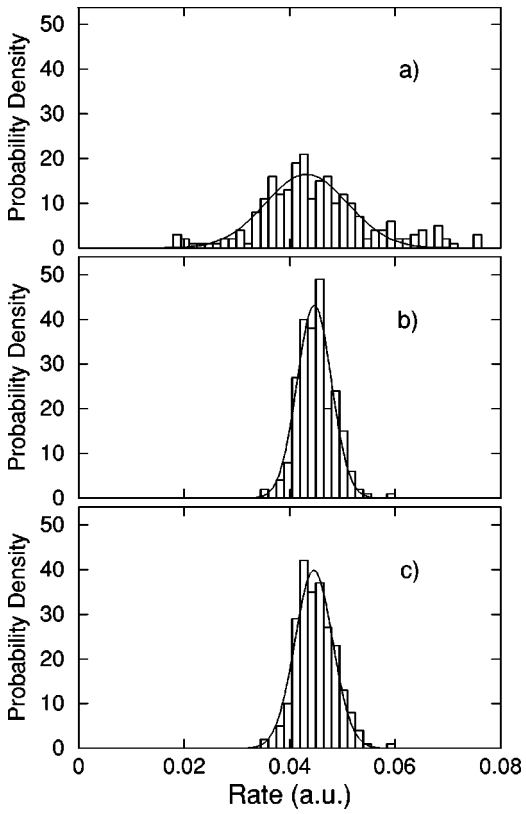

FIG. 5. Distribution of the autoionization rates. The Hartree-Fock rates γ_i^0 are shown in (a), γ_i in (b), and Γ_i in (c). The solid curves are Gaussian fits to the distributions.

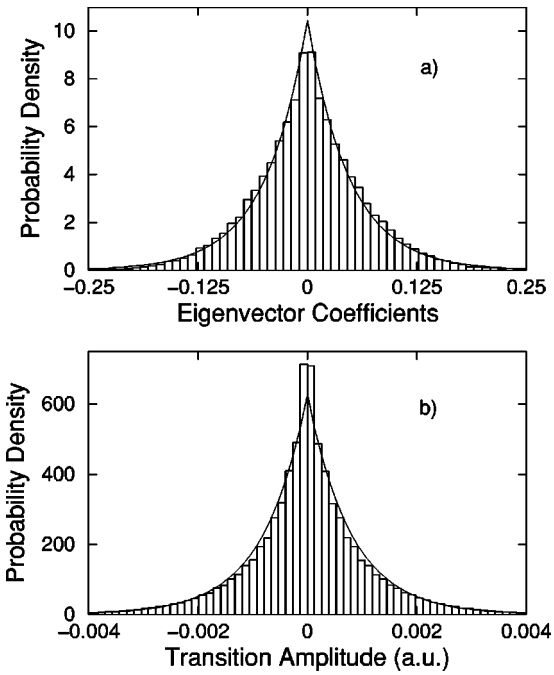

FIG. 6. Normalized distribution of the eigenvector coefficients of the matrix **h** (a) and the elements of the transition matrix **V** (b). The solid curve is the distribution $P(x)=1/(2D)\exp(-|x|/D)$, with $2D=0.096$ and $2D=0.0016$ a.u., respectively, for (a) and (b).

so that for uncorrelated channels, in the limit of $K \gg N$, the widths of the resonances can be obtained from perturbation theory, even if the resonances are strongly overlapping. The large number of channels effectively averages out interferences between the channels, resulting in the essentially incoherent decay of the hollow atomic states.

The mean and standard deviation of the off-diagonal matrix elements of $\mathbf{w}^{(0)}$ are 8.5×10^{-7} a.u. and 3.5×10^{-4} a.u., respectively. By comparison, the mean and standard deviation of the diagonal matrix elements of $\mathbf{w}^{(0)}$ are 2.3×10^{-2} a.u. and 5.3×10^{-3} a.u., respectively. This indicates that the approximations (4.7) and (4.8) should apply. Before comparing the approximate complex eigenvalues with the eigenvalues obtained by solving the eigensystem (3.6), let us consider the distribution of the rates $\gamma_i^{(0)}$ and γ_i. These are shown in Figs. 5(a) and Fig. 5(b), respectively. With the approximation that transitions to all the channels are equiprobable, Porter and Thomas [45] have shown that the distributions of the resonance widths are given by a χ^2 distribution with the number of degrees of freedom equal to the number of decay channels. For a large number of channels, the distribution of widths tends to a Gaussian. Clearly, for the system investigated here, this equiprobable channel approximation is not applicable. However, we make two observations. First, the distribution of the rates $\gamma_i^{(0)}$ and γ_i is well modeled by a Gaussian, as can be seen in Fig. 5. Second, a direct consequence of the equiprobable channel model is that the variance of the distribution of the rates is inversely proportional to the number of channels [46]. The strong mixing between the Hartree-Fock levels results in the transition amplitude matrix **V** having practically no zero elements. In fact, the matrix elements **V** are distributed in the same way as the eigenvector coefficients $c_{i,j}$, as shown in Fig. 6. This implies that each autoionization level can decay via all of the open channels and that, on average, the number of accessible channels increases by a factor of 6.8 compared with the zeroth-order approximation. From Table I, we see that the variance of the distribution of γ_i is about a factor of 5.5 smaller than the variance of the distribution of $\gamma_i^{(0)}$ (if the variances obtained from the Gaussian fit are used). Considering the simplicity of the equiprobable channel model, this agreement is noteworthy. However, many channels do not

TABLE I. Statistical parameters for the distributions of the rates $\gamma_i^{(0)}$, γ_i, and Γ_i.

Rate	Mean (a.u.)	Std. dev. (a.u.)	Variance	Variance (fit)	$\overline{K}$	$\overline{K}_{\text{effective}}$
$\gamma_i^{(0)}$	4.5×10^{-2}	1.1×10^{-2}	1.1×10^{-4}	6.0×10^{-5}	731	424
γ_i	4.5×10^{-2}	3.4×10^{-3}	1.2×10^{-5}	1.1×10^{-5}	4980	2082
Γ_i	4.5×10^{-2}	3.6×10^{-3}	1.3×10^{-5}	1.3×10^{-5}		

contribute significantly to the rates. If we omit these channels, under the constraint that the mean and standard deviation remain the same up to two significant figures, we obtain an effective average number of channels, $\overline{K}_{\text{effective}}$, given in Table I. Using these values for the effective number of channels, the number of channels increases by a factor of 4.9, which is in somewhat better agreement with the ratio of the variances of the widths $\gamma_i^{(0)}$ and γ_i obtained from the Gaussian fits.

The fact that the variance of the distribution of the widths $\gamma_i^{(0)}$ is greater than the variance of the distribution of the widths γ_i can be understood from Eqs. (4.6) and (4.7). Since

$$\gamma_i = \sum_{j=1}^{N} |c_{i,j}|^2 \gamma_j^{(0)}, \tag{4.9}$$

we see that the widths γ_i are simply a weighted average of the Hartree-Fock widths.

Finally, we discuss the distribution of the real and imaginary parts of the eigenvalues $\mathcal{E}_i$ of $\mathcal{H}$. As a consequence of Eq. (4.6), the distributions are expected to be similar to the distributions of ϵ_i and γ_i, respectively. We have already noted that the mean level spacings of the energies E_i and ϵ_i are the same. In Fig. 1, differences can be seen between the two distributions; however, they are not statistically significant. Table I gives the mean and standard deviation of the distributions of γ_i and Γ_i. The agreement between the two sets of parameters is very good, thereby confirming the validity of Eq. (4.8).

V. CONCLUSIONS

We have investigated some of the statistical properties of the 237 hollow $1s^2 4\ell^5\, ^2P^o$ states of nitrogen. These resonant states are strongly overlapping and the number of decay channels is much larger than the number of states. We have shown that the latter fact results in a number of important simplifications in the description of the system. Specifically, the matrix $\mathbf{w}^{(0)}$, and hence the matrix $\mathbf{w}$, is to a good approximation diagonal. This has the consequence that, despite the widths of the states being much larger than the mean energy separation, the widths can be calculated using perturbation theory. This, in turn, implies that the usual techniques for describing the spectra of closed systems, in particular, the GOE, can be applied to study the properties of the positions of the resonant states. This is in sharp contrast to the situation in which the number of channels is smaller than the number of resonant states. In this case, trapped states appear, which have been studied extensively within a number of contexts [34,47–52]. In addition, our results suggest that a further simplification can be made when determining the distribution of level widths. The mean width of the states can be obtained from the Hartree-Fock widths, which are approximately Gaussian distributed, with the variance of the distribution then corrected by a factor equal to the ratio of the nonzero channels to the total number of channels. This simple approximation can be tested by considering other strongly interacting systems that decay via a large number of open channels.

Our results predict that lifetimes of the quintuply excited states $1s^2 4\ell^5\, ^2P^o$ range between 5×10^{-16} and 6×10^{-16} s. Previous theoretical calculations, performed in an average-of-configuration approximation without taking into account correlation effects or the overlap between the resonances, predicted results of the same order of magnitude but with a larger spread in the distribution of lifetimes [11]. The effect of correlation was estimated and the conclusion reached that it does not change the average autoionization decay rates, but only reduces the variation of the widths. The present statistical analysis confirms this result. Vaeck and Hansen [11] also showed that their results did not depend on the number of core electrons in the system and predicted almost the same lifetime for the $1s^2 4\ell^5$ configuration as for the $1s4\ell^6$ configuration in N. If this is true, in general, we can compare our results with the only available experimental lifetime, 5×10^{-16} s, obtained for collisions of N^{6+} with Au at 600 eV [53]. However, it should be emphasized that this lifetime has been extracted from the measurement of the total number of electrons emitted while the ion and the metallic target interact. On average, about 19 Auger processes occur, with the exact distribution of the electrons in the excited shells not being known and the effect of the proximity of the surface difficult to estimate.

Experimental studies of hollow atoms produced by electron transfer during collision processes cannot provide precise information concerning the Auger decay of these states. However, the development of new generation light sources will allow hollow atoms to be studied in more detail. Recently, the hollow lithium $2s^2 2p\, ^2P^o$ state was observed using synchrotron photoexcitation [54]. This work initiated a large number of measurements of triply excited states up to the $(3\ell)^2 5\ell$ Rydberg series [55–59]. The new X-ray Free Electron Laser [60] facility will provide light of unprecedented frequencies and intensities, thereby creating new opportunities for spectroscopy of hollow atoms.

[1] J.P. Briand, L. de Billy, P. Charles, S. Essabaa, P. Briand, R. Geller, J.P. Desclaux, S. Bliman, and C. Ristori, Phys. Rev. Lett. **65**, 159 (1990); Phys. Rev. A **43**, 565 (1991).

[2] A. Arnau, F. Aumayr, P.M. Echenique, M. Grether, W. Heiland, J. Limburg, R. Morgenstern, P. Roncin, S. Schippers, R. Schuch, N. Stolterfoht, P. Vaga, T.J.M. Zouros, and H.P. Winter, Surf. Sci. Rep. **27**, 113 (1997).

[3] H.P. Winter and F. Aumayr, J. Phys. B **32**, R39 (1999).

[4] S. Ninomiya, Y. Yamazaki, F. Koike, H. Masuda, T. Azuma, K. Komaki, K. Kuroki, and M. Sekiguchi, Phys. Rev. Lett. **78**, 4557 (1997).

[5] P. Benoit-Cattin, A. Bordenave-Montesquieu, M. Boudjema, A. Gleizes, S. Dousson, and D. Hitz, J. Phys. B **21**, 3387 (1988).

[6] M. Barat and P. Roncin, J. Phys. B **25**, 2205 (1992).

[7] A. Delon, S. Martin, A. Denis, Y. Ouerdane, M. Carré, J.

Désesquelles, and M.C. Buchet-Poulizac, Radiat. Eff. Defects Solids **126**, 337 (1993).
[8] U. Thumm, Phys. Rev. A **55**, 479 (1997).
[9] A. Bárány and C.J. Setterlind, Nucl. Instrum. Methods Phys. Res. B **98**, 184 (1995).
[10] S. Martin, L. Chen, A. Denis, and J. Désesquelles, Phys. Rev. A **57**, 4518 (1998).
[11] N. Vaeck and J.E. Hansen, J. Phys. B **28**, 3523 (1995).
[12] C.E. Porter, *Statistical Theories of Spectra*: *Fluctuations* (Academic Press, New York 1965).
[13] T.A. Brody, J. Flores, J.B. French, P.A. Mello, A. Pandey, and S.S.M. Wong, Rev. Mod. Phys. **53**, 385 (1981).
[14] T. Guhr, A. Müller-Groeling, and H.A. Weidenmüller, Phys. Rep. **299**, 189 (1998).
[15] *Quantum Chaos and Statistical Nuclear Physics*, edited by T.H. Seligman and H. Nishioka (Springer, Berlin, 1986).
[16] V. Zelevinsky, Annu. Rev. Nucl. Part. Sci. **46**, 237 (1996).
[17] N. Rosenzweig and C.E. Porter, Phys. Rev. **120**, 1698 (1960).
[18] H.S. Camarda and P.D. Georgopulos, Phys. Rev. Lett. **50**, 492 (1983).
[19] L. Leviandier, M. Lombardi, R. Jost, and J.P. Pique, Phys. Rev. Lett. **56**, 2449 (1986).
[20] D.M. Leitner, H. Köppel, and L.S. Cederbaum, J. Chem. Phys. **104**, 434 (1996).
[21] R. Georges, A. Delon, and R. Jost, J. Chem. Phys. **103**, 1732 (1995).
[22] O. Bohigas, M.J. Giannoni, and C. Schmit, Phys. Rev. Lett. **52**, 1 (1984).
[23] F. Haake, *Quantum Signature of Chaos* (Springer-Verlag, Berlin, 1992).
[24] H.-J. Stöckmann, *Quantum Chaos*: *An Introduction* (Cambridge University Press, Cambridge, 1999).
[25] D. Delande and J.C. Gay, Phys. Rev. Lett. **57**, 2006 (1986).
[26] H. Friedrich and D. Wintgen, Phys. Rep. **183**, 37 (1989).
[27] H. Hasegawa, M. Robnik, and G. Wunner, Prog. Theor. Phys. Suppl. **98**, 198 (1989).
[28] J. Zakrzewski, K. Dupret, and D. Delande, Phys. Rev. Lett. **74**, 522 (1995).
[29] M. Domke, K. Schulz, G. Remmers, G. Kaindl, and D. Wintgen, Phys. Rev. A **53**, 1424 (1996).
[30] J.M. Rost, K. Schulz, M. Domke, and G. Kaindl, J. Phys. B **30**, 4663 (1997).
[31] G. Tanner, K. Richter, and J.M. Rost, Rev. Mod. Phys. **72**, 497 (2000).
[32] R. Püttner, B. Grémaud, D. Delande, M. Domke, M. Martins, A.S. Schlachter, and G. Kaindl, Phys. Rev. Lett. **86**, 3747 (2001).
[33] V.V. Flambaum, A.A Gribakina, G.F. Gribakin, and M.G. Kozlov, Phys. Rev. A **50**, 267 (1994).
[34] V.V. Flambaum, A.A. Gribakina, and G.F. Gribakin, Phys. Rev. A **54**, 2066 (1996).
[35] V.V. Flambaum, G.F. Gribakin, and F.M. Izrailev, Phys. Rev. E **53**, 5729 (1996).
[36] V.V. Flambaum, A.A Gribakina, and G.F. Gribakin, Phys. Rev. A **58**, 230 (1998).
[37] G.F. Gribakin, A.A Gribakina, and V.V. Flambaum, Aust. J. Phys. **52**, 443 (1999).
[38] J.P. Connerade, I.P. Grant, P. Marketos, and J. Oberdisse, J. Phys. B **28**, 2539 (1995).
[39] G. O'Sullivan, P.K. Carroll, P. Dunne, R. Faulkner, C. McGuinness, and N. Murphy, J. Phys. B **32**, 1983 (1999).
[40] F.H. Mies, Phys. Rev. **175**, 164 (1968).
[41] R.D. Cowan, *The Theory of Atomic Structure and Spectra* (University of California Press, Berkeley, 1981).
[42] H.W. van der Hart, N. Vaeck, and J.E. Hansen, J. Phys. B **27**, 3489 (1994).
[43] H.W. van der Hart, N. Vaeck, and J.E. Hansen, J. Phys. B **28**, 5207 (1995).
[44] B.G. Wilson, F. Rogers, and C. Iglesias, Phys. Rev. A **37**, 2695 (1988).
[45] C.E. Porter and R.G. Thomas, Phys. Rev. **104**, 483 (1956).
[46] V.V. Sokolov and V.G. Zelevinsky, Nucl. Phys. A **504**, 562 (1989).
[47] P. Kleinwächter and I. Rotter, Phys. Rev. C **32**, 1742 (1985).
[48] V.B. Pavlov-Verevkin, Phys. Lett. A **129**, 168 (1988).
[49] F. Remacle, M. Munster, V.B. Pavlov-Verevkin, and M. Desouter-Lecomte, Phys. Lett. A **145**, 265 (1990).
[50] I. Rotter, Rep. Prog. Phys. **54**, 635 (1991).
[51] M. Desouter-Lecomte and F. Culot, J. Chem. Phys. **98**, 7819 (1993).
[52] M. Desouter-Lecomte, J. Liévin, and V. Brems, J. Chem. Phys. **103**, 4524 (1995).
[53] M. Vana, F. Aumayr, C. Lemell, and H.P. Winter, Int. J. Mass Spectrom. Ion Processes **149/150**, 45 (1995).
[54] L. Kierman, E.R. Kennedy, J.-P. Mosnier, J.T. Costello, and B.F. Sonntag, Phys. Rev. Lett. **72**, 2359 (1994).
[55] Y. Azuma, F. Koike, J.W. Cooper, T. Nagata, G. Kutluk, E. Shigemasa, R. Wehlitz, and I.A. Sellin, Phys. Rev. Lett. **79**, 2419 (1997).
[56] Y. Azuma, S. Hasegawa, F. Koike, G. Kutluk, T. Nagata, E. Shigemasa, A. Yagishita, and I.A. Sellin, Phys. Rev. Lett. **74**, 3768 (1995).
[57] L. Kierman, M.K. Lee, B.F. Sonntag, P. Sladeczek, P. Zimmermann, E.T. Kennedy, J.-P. Mosnier, and J.T. Costello, J. Phys. B **28**, L161 (1995).
[58] L. Journel, D. Cubaynes, J.M. Bizau, S. Al Moussalami, B. Rouvellou, F.J. Wuilleumier, L. VoKy, P. Faucher, and A. Hibbert, Phys. Rev. Lett. **76**, 30 (1996).
[59] S. Diehl, D. Cubaynes, J.-M. Bizau, L. Journel, B. Rouvellou, S. Al Moussalami, F.J. Wuilleumier, E.T. Kennedy, N. Berrah, C. Blancard, T.J. Morgan, J. Bozek, A.S. Schlachter, L. VoKy, P. Faucher, and A. Hibbert, Phys. Rev. Lett. **76**, 3915 (1996).
[60] X. Andruszkow *et al.*, Phys. Rev. Lett. **85**, 3825 (2000).